

# **Studies on Large Mode Area and Long-Period Grating Assisted Microstructured Optical Fiber Devices**

**Synopsis of thesis submitted by**

**Annesha Maity**

**In partial fulfilment of the requirements for the degree of**

**Doctor of Philosophy**

**Under the supervision of**

**Dr. Shailendra K. Varshney**



**Department of Electronics and Electrical Communication Engineering  
Indian Institute of Technology,  
Kharagpur – 721302, India**

July 2014

## 1. Introduction and literature review

Light guidance in microstructured optical fibers is governed by the wavelength-scale manipulations in waveguide geometry that opens up the possibility for a number of unique and useful optical properties, unachievable through the conventional optical fibers. These fibers can be broadly classified into two groups: index-guiding and photonic bandgap guiding (PBG). Photonic crystal fibers (PCFs) are a subset of index-guiding microstructured fibers with a periodically structured cladding [1]; although a recently introduced microstructured core fiber (MCF) may also join this group in terms of periodically arranged high-index rods to form the core [2]. In MCFs, the modes in individual high-index rods couple evanescently to form a fundamental supermode that can possess a very large mode area suitable for high power delivery in fiber lasing and amplification [2]. Additionally, there exist scopes to modify/improve the design that may be utilized to obtain a low bend loss, as well, for practical usage. We resort to such design flexibility to get a large mode area, low bend loss and single mode MCF design (Section 4.1).

The remarkable advantages of PCFs include single mode operation over a wide range of wavelengths [3], large mode area [4], tailorable dispersion properties [1] and nonlinear effects [1]. The microstructure, even permits light guidance through air, known as the PBG, thus bypassing the glass-related attenuation and nonlinearities [1]. Additionally, the air-holes can be infiltrated with liquids/gases, altogether providing a number of new and improved applications in fiber optic sensing domain [5]. In the field of sensing, PCFs have shown a great promise in measuring physical parameters such as strain or surrounding refractive index (SRI); and among which the long period grating (LPG) structures inscribed in PCFs have drawn tremendous attention due to their simplicity [6-9]. However, as a physical sensor, these reports typically quote strain and SRI sensitivities in the range  $\sim 0.4\text{--}8$  nm/m $\epsilon$  [6-7] and 400–1300 nm/RIU [9], respectively. Furthermore, the temperature sensitivities of PCF-based LPGs [6] are almost two-orders of magnitude less than those of conventional fibers due to their pure silica structure. To obtain enhanced sensitivity from LPG-based devices, some authors have employed coupling to higher-order cladding modes leading to a phenomenon of dual resonance [10]. The dual resonance causes coupling to the same cladding mode at two distinct wavelengths which shifts in opposite directions with any change in external measurand. Measuring the separation between the dual peaks largely magnifies the sensitivity as shown in Ref. [11]. The approach has been employed in this work to obtain a high-performance sensor (Section 4.2).

The pure silica structure of PCFs contributes to its temperature insensitivity [6] that can be exploited to obtain various temperature-invariant devices. For example, erbium doped fiber amplifiers (EDFAs) which are attractive for wavelength division multiplexed (WDM) systems due to wide gain spectrum (1530 nm – 1570 nm), do not provide equal gain at all signal wavelengths and the gain spectrum must be flattened to evenly distribute power among all WDM channels. This is usually done with long period gratings [12-13]. Nonetheless, the temperature sensitivity of conventional fiber LPGs necessitates keeping the EDFA temperature constant to maintain the flattened gain profile in varying environments. In contrast to active temperature compensation, passive schemes are attractive in terms of system cost. At this point, a passively athermalized gain flattening filter from all-silica PCF can be promising, as described in Section 4.3 of this work.

## **2. Motivation**

Throughout the past, there have been numerous efforts on the development of large mode area fibers [2] aiming towards high power delivery. However, these attempts also face challenges from high bending losses. A novel fiber design with both large mode area and low bending loss is highly desirable. In this aspect, we have attempted to achieve the goal employing a recently known fiber called the MCF. This has been described in Section 4.1.

A thorough literature survey reveals the abundance of researches pertaining to endlessly single-mode PCFs [6, 8] or the fundamental mode of a PCF [7], however studies on the second-order mode of dual mode PCFs are very few. So the present scenario offers ample opportunities to explore all the aspects of a dual mode PCF. While going through such efforts, a particularly interesting feature in the second-order mode has been observed, which we have concluded to be a fascinating topic of research and is summarized in Section 4.2.

Even though all-silica PCFs are known to be temperature insensitive [6, 8], the possibility of these fibers as athermalized EDFA-gain flattening filter has not yet been explored. There has been a great demand throughout the years for a fiber amplifier with temperature-invariant gain spectrum that can operate in varying environments. In this respect, an all-silica PCF can serve as an excellent alternative and Section 4.3 attempts to meet this demand.

## **3. Objectives**

The overall objectives of the work presented in the thesis are outlined below:

- (i) The microstructure in fibers, like MCFs, offers a great deal of design flexibility, which can be utilized to obtain a large mode area fiber. Again, the techniques such

as placing a low index trench in the cladding to mitigate bend losses have been known. So the combination of these two approaches has the possibility to meet our present demand.

- (ii) The unusual characteristics of the second-order mode in the PCF considered, promise the dual resonance phenomenon. Such dual resonance can give us a high performance sensor considering the peak separation sensing approach, first proposed in [10]. Further, due to the independent nature of the dual peaks, the concept can also be utilized for simultaneous strain/temperature sensing.
- (iii) Once again, the microstructure in PCFs can be exploited to meet some of the important requirements of a fiber amplifier, namely, a short length amplifying module and low splice loss with conventional step index fibers. The amplifier gain spectrum can be flattened for possible uses in WDM systems, using the standard techniques. These features when clubbed with the temperature-insensitivity of all-silica PCFs, promise an efficient fiber amplifier with temperature-invariant gain spectrum.

## 4. Work carried out and some representative results

### 4.1. Large mode area, low bend loss, single mode microstructured fiber

A microstructured core fiber (MCF) is a recently introduced fiber structure [2] comprising of Ge-doped silica rods of diameter  $d$ , arranged hexagonally to form a lattice with rod-to-rod spacing (lattice constant or pitch) of  $\Lambda$ . This core geometry is embedded in a low-index silica cladding. The small rods compared to operating wavelength cause the individual rod-modes to couple and form a fundamental supermode. Such fiber structure with its design parameters is shown in Fig. 1(a). The microstructured core in MCFs can be replaced with an equivalent core similar to a step index fiber and its index as the effective index of the fundamental space filling mode (FSM), which has been determined by full-vectorial effective index method. The guided mode index is then deduced from the standard step index fiber eigenvalue equation. The dispersion of guided mode indices as a function of the number of rings of high-index rods, is shown in Fig. 1(b). The mode-formation mechanism in MCF indicates a possibility to use it as a large mode area, single mode fiber subject to the design constraints. The quantity that ensures single-modedness is the V-parameter which is defined for MCF as,

$$V_{eff} = \frac{2\pi}{\lambda} a_{eff} \sqrt{(n_{co}^{FSM})^2 - n_{sil}^2} \quad \dots(1)$$

where,  $a_{eff}$  is the radius of the equivalent core of the MCF,  $n_{co}^{FSM}$  is the effective index of the FSM and  $n_{sil}$  is the silica refractive index.

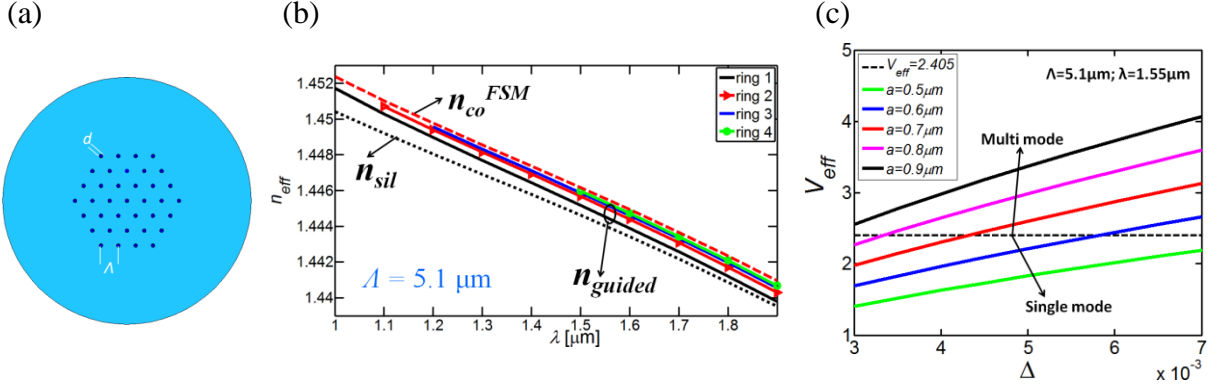


Fig.1: (a) Schematic cross section of MCF, (b) Effective mode indices of the fundamental mode as a function of wavelength for different number of rings, (c) Variation of V-parameter of the MCF with relative index difference ( $\Delta$ ) and individual rod radii ( $a$ ).

Figure 1(c) shows that increasing the index difference ( $\Delta = \frac{n_r^2 - n_{sil}^2}{2n_r^2}$ ,  $n_r$  is the rod index)

between rods and silica increases the effective core index  $n_{co}^{FSM}$  and hence the effective V-parameter  $V_{eff}$ . Similarly, by increasing the individual rod radii ( $=d/2$ ), the field confines more within the rods, thus pushing  $n_{co}^{FSM}$  more towards the refractive index of the rods and hence increases  $V_{eff}$ . In addition, a large pitch  $\Lambda$  shrinks the fields more within rods, thereby increasing  $V_{eff}$ . We observe that the MCF is operable in single mode regime for small values of  $a$ ,  $\Lambda$  and  $\Delta$  at a particular wavelength. The effective mode area of the fundamental supermode is defined by:

$$A_{eff} = \frac{\left[ \int_{-\infty}^{\infty} \int_{-\infty}^{\infty} \psi^2(r, \phi) r dr d\phi \right]^2}{\int_{-\infty}^{\infty} \int_{-\infty}^{\infty} \psi^4(r, \phi) r dr d\phi} \quad \dots(2)$$

where,  $\psi(r, \phi)$  is the cross-sectional distribution of the fundamental mode,  $r$  and  $\phi$  are the radial and azimuthal coordinates, respectively. Fig. 2(a) shows three dimensional plot of  $A_{eff}$  with respect to normalized radius  $a/\Lambda$  and normalized wavelength  $\lambda/\Lambda$  for  $\Delta$ : 0.3%. It is possible to realize effective mode area greater than  $2000 \mu\text{m}^2$  at 1550 nm for small values of  $a$  and  $\Delta$ , at the cost of high bending loss (BL). To reduce the bend losses, we have introduced two improved MCF designs, namely, trench-assisted MCF (TAMCF) and hole-assisted MCF (HAMCF), as sketched in Figs. 2(b) and 2(c), respectively. The TAMCF has been examined under three trench positions: (i) *closer to core*, (ii) *slightly away from core* and (iii) *moderate*

distance from core. Fig. 3(a) shows the fundamental mode profile of the TAMCF for case (ii)-trench position and bent in x-plane under standard packaging radius of 7.5 cm with  $A_{eff} \sim 1300 \mu\text{m}^2$  and BL  $< 0.1$  dB/m. Figure 3(b) shows the mode profile for HAMCF with bending radius of 5 cm. Figures 3(c) and 3(d) plot, respectively, the mode-area and the BL as a function of bending radius. It is evident that, although HAMCF is more bend-insensitive, the TAMCF is a good choice for attaining large  $A_{eff}$  ( $> 1000 \mu\text{m}^2$ ) with acceptable BL ( $< 0.1$  dB/m) under standard packaging radii.

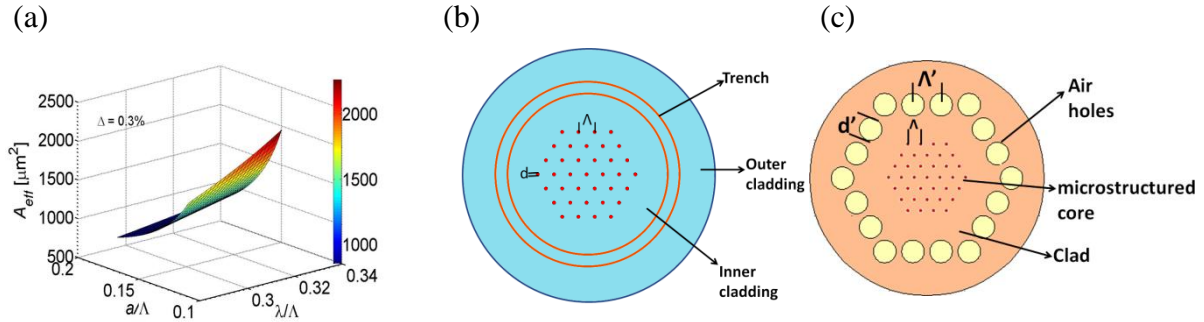


Fig. 2: (a) Effective mode area ( $A_{eff}$ ) as a function of normalized rod radii ( $d/\lambda$ ) and normalized wavelength ( $\lambda/\lambda$ ), (b) Trench-assisted MCF and (c) Hole-assisted MCF designs for large mode area with low bend loss.

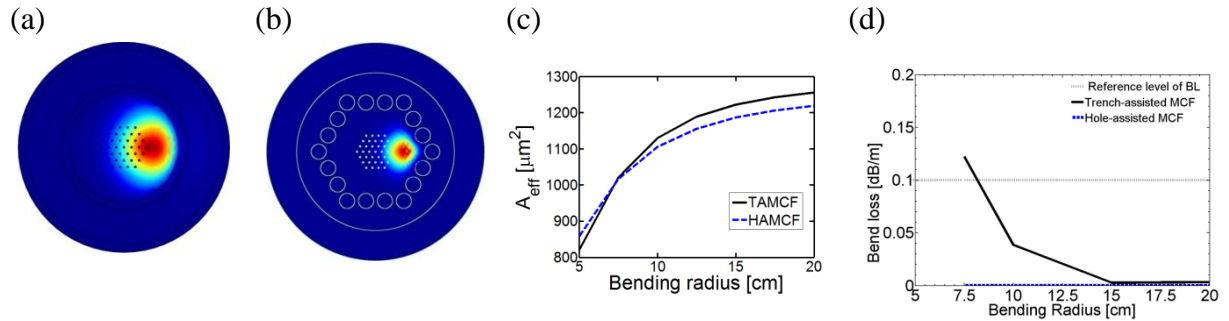


Fig.3: Fundamental mode profiles of (a) TAMCF with trench placed at moderate distance and (b) HAMCF, under bend radii of 7.5 cm and 5 cm, respectively, in x-plane. (c)  $A_{eff}$  as a function of bend radius for TAMCF and HAMCF (d) Bend loss of TAMCF and HAMCF as a function of bending radius.

#### 4.2. Highly sensitive long period grating inscribed photonic crystal fiber sensor

This section is devoted to study on LPG inscribed in a Ge-core, dual-mode PCF where the second-order core mode ( $LP_{11}$ ) exhibits a non-monotonicity in its phase matching curve (PMC) that leads to a dual resonance feature. Finite element method based numerical simulations reveal that dual peaks separate by 180 nm when 2 mε strain is applied and by 170 nm with a 275 °C rise in temperature, which are much higher than the shift observed in single resonance peaks. It has also been found that due to relatively small cladding radius of the

same fiber, the fundamental mode ( $LP_{01}$ ) shows a peak shift of 1848 nm/RIU when surrounding refractive index (SRI) changes from 1.325 to 1.35. The LPG characteristic curve or the PMC is constructed using the phase matching condition,

$$\lambda_r = \Lambda_g \left( n_{eff}^{co} - n_{eff}^{cl} + \frac{\kappa_{co-co} - \kappa_{cl-cl}}{k} \right) \quad \dots(3)$$

where,  $\lambda_r$  denotes the phase-matched or resonance wavelength and  $\Lambda_g$  is the LPG period,  $n_{eff}^{co}$  and  $n_{eff}^{cl}$  are, respectively, the effective indices of core and cladding modes,  $k$  is the free-space wave number,  $\kappa_{co-co}$  and  $\kappa_{cl-cl}$  are the self-coupling coefficients of the core and cladding modes, respectively. The non-monotonic PMC of the  $LP_{11}$  mode is shown in Fig. 4(a) along with the simulated fiber cross-section in inset.

Application of a small axial strain ( $\varepsilon$ ) to the fiber increases the LPG period by  $\Delta\Lambda_g = \varepsilon\Lambda_g$ . The PMC changes due to the strain-optic coefficients ( $dn/d\varepsilon$ ) of the fiber materials and we get new phase matching points as shown in Fig. 4(b). The corresponding loss characteristics of the LPG are shown in Fig. 4(c) with an estimate of peak separation in inset. The peak separation is as high as 180 nm under 2 mε of applied strain.

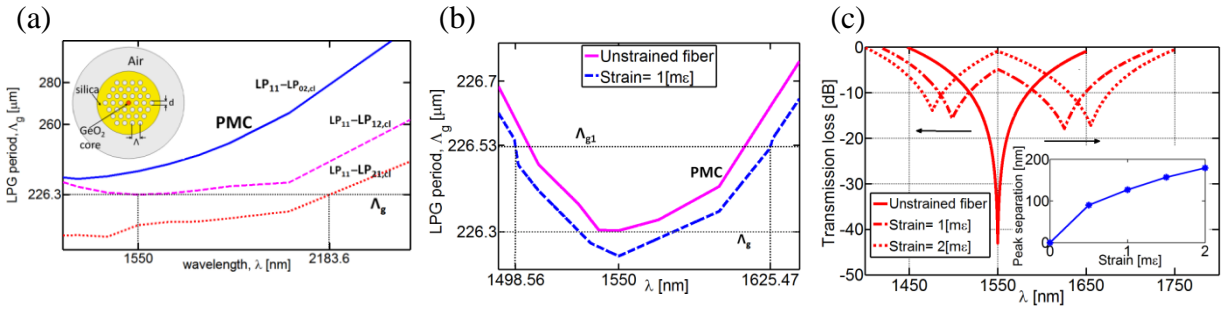


Fig. 4: (a) Non-monotonic PMC of  $LP_{11}$  with the resonating  $LP_{12}$ -like cladding mode, inset: schematic cross-section of the simulated dual-mode PCF, (b) two resonance wavelengths due to 1 mε strain and (c) loss profile evolution of the  $LP_{11}$ -associated LPG with varying strain.

The PMC in response to temperature behaves similarly as in strain case and records a peak separation of 170 nm with 275 °C rise from the room temperature (25 °C). These results are much better than the calculated shifts of single resonance peaks in the LPG associated with  $LP_{01}$  mode. Notably, computation on temperature response has proceeded with the thermal expansion ( $\alpha = d\Lambda_g / \Lambda_g dT$ ) of grating pitch and the thermo-optic coefficient ( $dn/dT$ ) of the fiber materials. The response to SRI of  $LP_{11}$ -associated LPG has deviated from strain/temperature responses and we do not achieve any dual resonance behaviour in this case. However, due to a relatively small cladding radius (20.5 $\mu\text{m}$ ), the single resonance

peaks of the LP<sub>01</sub>-associated LPG record a shift of 1848 nm per refractive index units when SRI changes from 1.325 to 1.35. This has been shown in Fig. 5(a). A study on dual resonance peaks reveals the independent response of these two peaks to both strain and temperature, allowing us to design a simultaneous strain-temperature sensor. The applied strain and temperature can be obtained from the matrix equation,

$$\begin{pmatrix} \Delta\varepsilon \\ \Delta T \end{pmatrix} = \frac{1}{\Delta} \begin{pmatrix} S_{T2} & -S_{T1} \\ -S_{\varepsilon2} & S_{\varepsilon1} \end{pmatrix} \begin{pmatrix} \Delta\lambda_1 \\ \Delta\lambda_2 \end{pmatrix} \quad \dots(4)$$

where,  $S_{\varepsilon1}$ ,  $S_{\varepsilon2}$ ,  $S_{T1}$ ,  $S_{T2}$  are the respective strain and temperature sensitivities of each peak that are obtained slopes of peak-shifts with  $\varepsilon$  or  $T$ , like the one described in Figs.5(b)–5(c). The determinant of the sensitivity matrix in eq.(4) is 16.1857, which is considerable to minimize any errors in recovering strain and temperature. For example, in a system with detector resolution of 1 pm, the maximum recovery errors are 0.067  $\mu\varepsilon$  and 0.0057  $^{\circ}\text{C}$ , which are much better than the reported systems in [14,15].

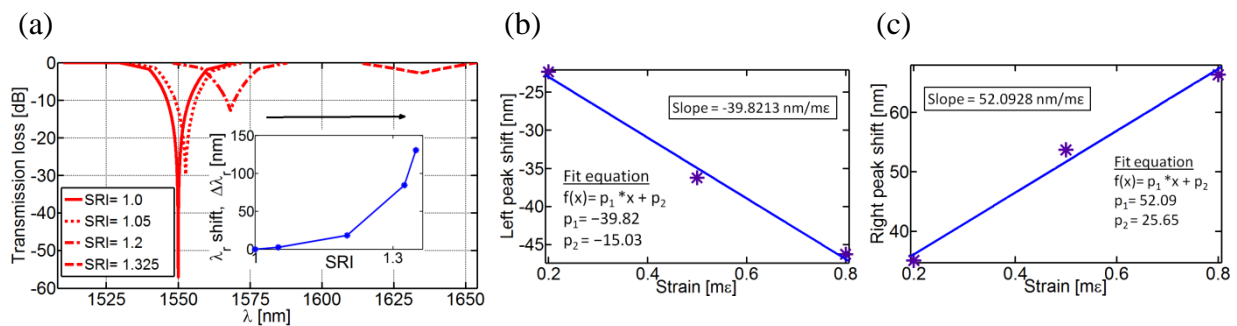


Fig.5: (a) Loss profile evolution of the LP<sub>01</sub>-associated LPG with varying strain (b),(c) strain-sensitivity calculations of the left and right resonance wavelength peaks, respectively.

### 4.3. Temperature-insensitive, gain-flattened Erbium-doped photonic crystal fiber amplifier

The well-established temperature insensitivity [6] of all-silica PCFs has been employed in this work to get a passively athermalized gain flattening filter. Besides, the added advantages of using PCF as a host amplifying fiber are: (i) the “active” core size can be increased to attain high overlap factor for shorter module length, while still maintaining single modedness and (ii) the PCF-pitch can be adjusted suitably to yield a compatible mode area with conventional fibers, thus giving low splice loss. Based on observations of mode fields which spread over a minimum region of space, we have proposed to enlarge the core to encompass the mode-field area sufficiently. This increases the overlap factor significantly, as can be visualized from Figs. 6(a) and 6(b). Additionally, increasing the first ring hole radii can repel

the fields towards the core and further augmenting the overlap factor. A design of such PCF with optimized parameters is shown in Fig. 6(c). The optimized pitch ( $\Lambda$ ) of  $9\ \mu\text{m}$  gives very low splice loss ( $\sim 5 \times 10^{-4}$  dB) due to sufficiently matching mode area. Amplifying property of this designed fiber is obtained by solving the well-known population rate equations and the propagation equations. The optimum length,  $L_{\text{opt}}$  of the amplifier with 190 mW pump power and  $1\ \mu\text{W}$  signal power, is obtained 11.15 m. This result may be compared to [16] where  $L_{\text{opt}}$  is greater (31 m), opposed to only 10.7 m in our design for input pump and signal powers of 190 mW and  $1.67\ \mu\text{W}$ , respectively.

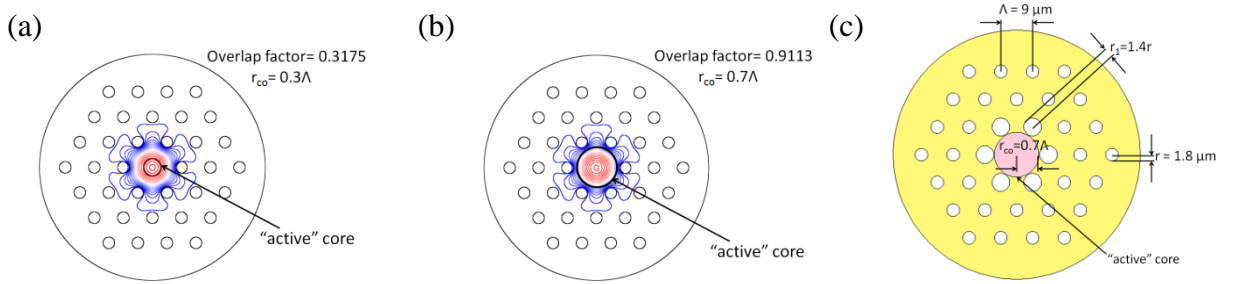


Fig.6: (a), (b) provide illustrations of increase in overlap factor with increasing doped core radius, (c) PCF design for high overlap factor and compatible mode area.

Gain spectrum obtained for the designed PCF is shown in Fig. 7(a) which contains three distinct peaks, suppression of which using a single LPG is not possible as it provides only one rejection dip. In this respect, an elegant method that uses a LPG closely spaced with a phase-shifted LPG (PSLPG), as reported in [13], can be beneficial. A PSLPG contains an unperturbed region in its periodic index modulation which has been combined with PCF to attain flattened gain spectrum with ripples of 0.58 dB over a bandwidth of 27.5 nm. The optimized loss profiles of the LPG and PSLPG are given in Fig. 7(b) and the flattened spectrum in Fig. 7(c). The computed overlap factors that contribute to the gain spectrum, are found to change negligibly with temperature. This leaves the device to respond primarily to the shifts in LPG spectra against temperature. The shifts have been computed by considering  $dn/dT$  of silica and its thermal expansion  $\alpha$  which affects all the length attributes of the two gratings. The LPGs' loss profiles for three calculated temperatures ( $-20^\circ\text{C}$ ,  $20^\circ\text{C}$ ,  $60^\circ\text{C}$ ) and the corresponding flattened spectra are shown in Fig. 8(a) and Fig. 8(b), respectively. The LPG/PSLPG loss profiles do not shift ( $\sim 250\ \text{pm}/40^\circ\text{C}$  temperature change) significantly with respect to temperature, as shown in Fig.5(a), due to all-silica structure of the PCF. Consequently, the ripples in the flattened spectrum are seen to change with maximum ripples of  $\sim \pm 0.57$  dB over the same bandwidth (27.5 nm) in the temperature range of  $80^\circ\text{C}$ . The result is comparable to that reported in [17] realized by macro-bending of the fiber.

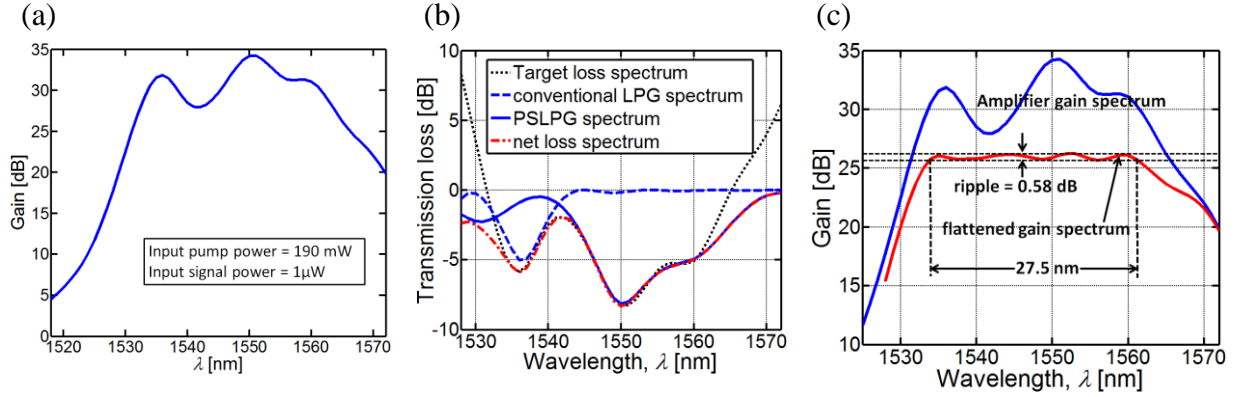


Fig.7: (a) Gain spectrum of the designed erbium doped PCF with 190 mW pump power and 1  $\mu$ W power for all signal wavelengths spanning over 1518 nm–1572 nm (b) optimized loss profiles of the LPG and PSLPG for flattening the gain spectrum and (c) flattened gain spectrum with 0.58 dB ripple over 27.5 nm.

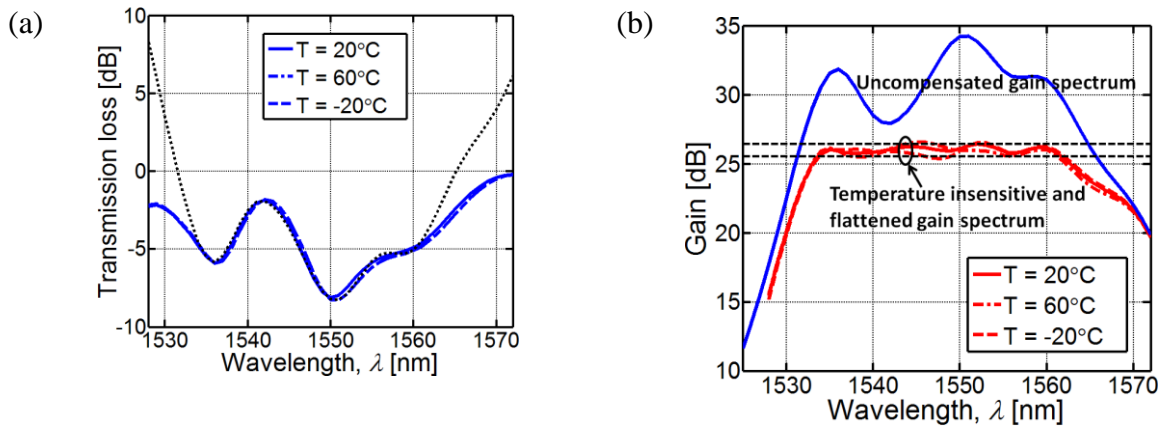


Fig.8: (a) The net loss profile at three temperature ranges ( $-20^{\circ}\text{C}$ ,  $20^{\circ}\text{C}$ ,  $60^{\circ}\text{C}$ ), (b) temperature insensitive and flattened gain spectrum of the designed erbium-doped PCF ( $d=3.6\mu\text{m}$ ,  $\Lambda=9\mu\text{m}$ ,  $r_1=2.52\mu\text{m}$ ,  $r_{co}=6.3\mu\text{m}$ ).

## 5. Summary

We have carried out to meet some of the objectives demanded by the present scenario. The work is fully analytical as well numerical. We have obtained some interesting results, among which some are summarized here. The detailed results shall be presented in the thesis.

## 6. Thesis Organization

A brief overview of the work carried out in the thesis and its organization is summarized below:

Chapter 1 presents a brief introduction on the microstructured fibers and their various application areas. A brief discussion on the numerical methods employed for the analysis of

these fibers is given. The various uses of microstructured fibers inscribed with gratings are discussed as well. Finally, the three novel microstructured fiber systems specific to some of the most demanding applications have been introduced, which are also the major outcomes of the work carried out in the thesis.

Chapter 2 gives a literature survey on different advantages and applications of microstructured fibers. The uniqueness of these fibers in achieving some of the most desired properties in the present scenario, are presented.

Chapter 3 describes in brief, a newly introduced fiber, the MCF. The modal properties and the dispersion characteristics of MCF have been numerically presented using FVEIM. The fiber has been investigated for large mode area under single-mode operation regime. The design has been modified and improved by introducing TAMCF and HAMCF; the former gives a larger mode area with acceptable bending loss at standard packaging radii, while still maintaining single-mode operation. The fiber can be useful for high power lasing and amplifying applications.

Chapter 4 proposes a novel high performance sensor based on a LPG-inscribed dual-mode PCF. The unusual behaviour of the phase matching characteristics of the higher-order mode in this fiber is exploited to obtain improved sensing properties. Further, a scheme for simultaneous strain and temperature sensing have been presented which is superior in comparison to many existing systems.

Chapter 5 proposes a novel PCF design aimed for short erbium-doped fiber amplifying module with considerably low splice loss when aligned with conventional step index fibers. The amplifier's gain spectrum has been flattened using a combination of a LPG and a PSLPG. The flattened gain spectrum has been insensitive to temperature due to the single material composition of the fiber. The amplifying device, thus proposed, can be useful for WDM systems operating under varying environmental conditions.

The final chapter (chapter 6) summarizes the important conclusions drawn from the thesis. The thesis concludes by suggesting the future scope of work.

## References

- [1] P. Russell, "Photonic crystal fibers," *Science*, vol. 299, pp. 358-362, 2003.
- [2] G. Canat, R. Spittel, S. Jetschke, L. Lombard, P. Bourdon, "Analysis of the multifilament core fiber using the effective index theory," *Opt. Exp.*, vol. 18, pp. 4644-4654, 2010.
- [3] T. A. Birks, J. C. Knight, P. St. J. Russell, "Endlessly single mode photonic crystal fiber," *Opt. Lett.*, vol. 22, pp. 961-963, 1997.
- [4] J. C. Knight, T. A. Birks, R. F. Cregan, P. St. J. Russell, J. P. De Sandro, "Large mode area photonic crystal fibre," *Electron. Lett.*, vol. 34, pp. 1347-1348, 1998.

- [5] O. Frazão, J. L. Santos, F. M. Araújo, L. A. Ferreira, "Optical sensing with photonic crystal fibers," *Las. Phot. Rev.*, vol. 2, pp. 449-459, 2008.
- [6] J. S. Petrovic, H. Dobb, V. K. Mezentsev, K. Kalli, D. J. Webb, I. Bennion, "Sensitivity of LPGs in PCFs fabricated by an electric to temperature, strain, and external refractive index," *J. Light. Tech.*, vol. 25, pp. 1306-1312, 2007.
- [7] Y-P. Wang, L. Xiao, D. N. Wang, W. Jin, "Highly sensitive long-period fiber-grating strain sensor with low temperature sensitivity," *Opt. Lett.*, vol. 31, pp. 3414-3416, 2006.
- [8] H. Dobb, K. Kalli, D. J. Webb, "Measured sensitivity of arc-induced long-period grating sensors in photonic crystal fibre," *Opt. Comm.*, vol. 260, pp. 184-191, 2006.
- [9] Y. Zhu, Z. He, H. Du, "Detection of external refractive index change with high sensitivity using long-period gratings in photonic crystal fiber," *Sens. Act. B*, vol. 131, pp. 265-269, 2006.
- [10] X. Shu, X. Zhu, Q. Wang, S. Jiang, W. Shi, Z. Huang, D. Huang, "Dual resonant peaks of LP<sub>015</sub> cladding mode in long-period gratings," *Electron. Lett.*, vol. 35, pp. 649-651, 1999.
- [11] X. Shu, X. Zhu, S. Jiang, W. Shi, D. Huang, "High sensitivity of dual resonant peaks of long-period fibre grating to surrounding refractive index changes," *Electron. Lett.*, vol. 35, pp. 1580-1581, 1999.
- [12] A. M. Vengsarkar, J. R. Pedrazzani, J. B. Judkins, P. J. Lemaire, N. S. Bergano, C. R. Davidson, "Long-period fiber-grating- based gain equalizers," *Opt. Lett.*, vol. 21, pp. 336-338, 1996.
- [13] M. Harumoto, M. Shigehara, H. Suganuma, "Gain-flattening filter using long-period fiber gratings," *J. Lightwave Tech.*, vol. 20 pp.1027-1033, 2002.
- [14] O. Frazão, J. P. Carvalho, L. A. Ferreira, F. M. Araújo, J. L. Santos, "Discrimination of strain and temperature using Bragg gratings in microstructured and standard optical fibers," *Meas. Sci. Technol.*, vol. 16, pp. 2109-2113, 2005.
- [15] D-P. Zhou, L. Wei, W-K. Liu, J. W. Y. Lit, "Simultaneous measurement of strain and temperature based on a fiber Bragg grating combined with a high-birefringence fiber loop mirror," *Opt. Comm.*, vol. 281, pp. 4640-4643, 2008.
- [16] S. Hilaire, D. Pagnoux, P. Roy, S. Février, "Numerical study of single mode Er-doped microstructured fibers: influence of geometrical parameters on amplifier performances," *Opt. Exp.*, vol.14, pp.10865-10877, 2006.
- [17] P. Hajireza, S. D. Emami, S. Abbasizargaleh, S. W. Harun, D. Kumar, H. A. Abdul-Rashid, "Temperature insensitive broad and flat gain C-band EDFA based on macro-bending," *Prog. Electromagn. Res.*, vol. 15, pp. 37-48, 2010.

## Publications

### Journals

- [1] B.L. Behera, **A. Maity**, S.K. Varshney and R. Datta "Theoretical investigations of trench-assisted large mode-area, low bend loss and single-mode microstructured core fibers," *Opt. Comm.*, vol. 307, pp.9-16, 2013.
- [2] **A. Maity** and S.K. Varshney "Ultrasensitive properties of long period grating inscribed in a dual mode photonic crystal fiber," *IEEE Sens.*, vol. 14, pp. 2833-2840, 2014.
- [3] **A. Maity** and S. K. Varshney, "Efficient erbium doped photonic crystal fiber design with athermalized gain flattening," (to be communicated).

### Conference Proceedings

- [1] **A. Maity** and S. K. Varshney "Modeling of Multifilament core fibers and its Propagation Characteristics," Photonics 2010, IIT Guwahati, India.
- [2] B.L. Behera, **A. Maity**, R. Datta and S.K.Varshney "Designing bend-limited large mode area multicore optical fibers," IQEC/CLEO Pacific Rim 2011, Sydney, Australia.
- [3] **A. Maity** and S. K. Varshney "Selective suppression of the fundamental mode in a dual-mode photonic crystal fiber," TP<sub>0,31</sub>, OSA Technical Digest (online), Photonics 2012, IIT Chennai, India.